Temperature-sensitive eIF5A Mutant Accumulates Transcripts Targeted to the Nonsense-mediated Decay Pathway*[S]

Rainer Schrader[‡1], Craig Young[‡], Detlef Kozian[§], Reinhard Hoffmann[¶], and Friedrich Lottspeich[‡]

From the [‡]Department for Protein Analytics, Max Planck Institute for Biochemistry, Am Klopferspitz 18, 82152 Martinsried, Germany, [§]Aventis Pharma Germany (GmbH), Brueningstrasse 50, 65929 Frankfurt, Germany, and [¶]Department of Bacteriology, Max von Pettenkofer Institute, Pettenkoferstrasse 9a, 80336 Munich, Germany

The highly conserved protein eIF5A found in Archaea and all eukaryotes uniquely contains the posttranslationally formed amino acid hypusine. Despite being essential the functions of this protein and its modification remain unclear. To gain more insight into these functions temperature-sensitive mutants of the human *EIF5A1* were characterized in the yeast *Saccharomyces cerevisiae.* Expression of the point mutated form V81G in a ΔeIF5A strain of yeast led to a strongly temperature-sensitive phenotype and to a significantly reduced protein level at restrictive temperature. The mutant showed accumulation of a subset of mRNAs that was also observed in nonsense-mediated decay (NMD)-deficient yeast strains. After short incubation at restrictive temperature the mutant exhibited increased half-lives of the intron containing *CYH2* pre-mRNA and mature transcripts of NMD-dependent genes. Reduced telomere silencing and shortening was detected in the V81G mutant further supporting similarities to NMD-deficient strains. Our data suggest that eIF5A mediates important cellular processes like cell viability and senescence through its effects on the stability of certain mRNAs.

The cellular physiology of mRNA processing, transport, localization, and turnover is central to the process of gene expression at the posttranscriptional level. Increasing evidence has been found for a close connection between mRNA degradation processes and the steps of translation. The highly conserved hypusine-containing protein eIF5A has been implicated in both of these aspects of RNA metabolism; however, its precise cellular function is not yet fully understood.

Hypusine formation is a two-step enzymatic reaction catalyzed by deoxyhypusine synthase and then deoxyhypusine hydroxylase (1). The disruption of genes encoding either eIF5A or deoxyhypusine synthase in yeast leads to a lethal phenotype (2)

demonstrating that the deoxyhypusine residue is essential for the function of eIF5A and thus for proliferation and cell survival. The genome of *Saccharomyces cerevisiae* contains two *HYP* genes (*HYP1*, alias *TIF51B* or *ANB1*, and *HYP2*, alias *TIF51A*) coding for eIF5A. These genes are differentially expressed under aerobic and anaerobic conditions (3) and share an identity of 90%. *HYP* genes of other higher eukaryotes, *e.g.* one of the two human *HYP* genes (encoding *EIF5A1*), can functionally replace these yeast-specific genes (4, 5).

The eIF5A protein was first isolated from rabbit reticulocyte lysate ribosomes and classified as a translation initiation factor because *in vitro* the protein enhanced the building reaction of the first peptide bond measured as the yield of methionine-puromycin (6). However, cell fractionation revealed that only a small fraction of the protein associated with ribosomes (7). Moreover depletion or inactivation of the protein in *S. cerevisiae* reduced the global protein synthesis rate by only 30% (8, 9). Thus, the role of eIF5A as a translation initiation factor remains to be confirmed.

eIF5A is an RNA-binding protein (10), and it was hypothesized to regulate the translation of a subset of mRNAs that are needed for G_1/S cell cycle progression because agents blocking deoxyhypusine hydroxylase (11) or deoxyhypusine synthase (12, 13) induced a cell cycle arrest at the G_1/S boundary in several mammalian cell types. These results were supported by the G_1 arrest at 37 °C of yeast cells expressing a temperature-sensitive point mutated form of Tif51A (14).

The finding that eIF5A is a cellular cofactor of human immunodeficiency virus type 1 Rev and human T-cell lymphotrophic virus type 1 Rex transactivator proteins in mRNA export and the interaction of eIF5A with the general exportin Crm1p for nuclear export signal-containing proteins in higher eukaryotes suggested it played a role in nucleoplasmatic shuttling of mRNA (15–17). However, although the protein was found to be located in the nucleus and the cytosol of COS-7 cells (18), active shuttling between both compartments could not be confirmed. Also a direct interaction between Rev and eIF5A has not been shown (19). In addition yeast strains expressing temperature-sensitive mutants of Crm1p did not show a mislocalization of eIF5A to the nucleus (20). Therefore the nuclear export hypothesis has been questioned.

The implication of eIF5A in mRNA degradation initially came from studies of a temperature-sensitive *HYP2* mutant (ts1159) that showed an accumulation and a strongly prolonged

---

TABLE 1
Yeast strains used in this study

Strain	Genotype	Source or Ref.
W303-1*MAT*a	*MAT*a, *leu2-3, 112, ura3-1, 112, his3-11, 15, trp1-l, 15, ade2-l, can1-100*	26
WDH#6-9[YEpHYP2]	*MAT*a, *hyp2::LEU2, HYP2, YEp (URA3)* else isogenic to W303-1*MAT*a	4
W303Δh1h2	*MAT*a, *hpy1::TRPI, hyp2::LEU2, HYP2, YEp (URA3)* else isogenic to W303-1*MAT*a	This study
WDHyp2-Gal	*MAT*a, *hyp1::TRPI, hyp2::LEU2, HYP2, pRS*	This study
WDH(hum)Gal	*MAT*a, *hyp1::TRPI, hyp2::LEU2, EIF5A1, pRS*	This study
WDHG$_{81}$Gal	*MAT*a, *hyp1::TRPI, hyp2::LEU2, EIF5A1-V81G, pRS*	This study
PLY118	*MAT*a *upf1-Δ1::URA3 ura3-52 trp1-7 leu2-3,112 2 his4-38*	27

TABLE 2
Plasmids used in this study

Plasmid	Description	Ref.
YEp352	*2μ, LacZ, amp, MCS, URA3*	28
YEpHYP2	YEp352 containing yeast wild-type *HYP2* including its genomic promoter (cloned as PstI fragment)	This study
pRS315	pBluescript, *LEU2, CEN6, ARSH4, AmpR, LacZ*	29
pRSG313	pRS313 containing the *GAL1* promotor fragment cloned EcoRI BamHI	3
pRSG316	pRS316 containing the *GAL1* promotor fragment cloned NotI SalI	This study
pRSG313-HYP2	pRSG313 expressing the yeast wild-type Hyp2p	3
pRSG313-EIF5A1	pRSG313 expressing human wild-type EIF5A1	This study
pRSG313-EIF5A1G$_{81}$	pRSG313 containing point mutated (V81G) human *EIF5A1* fragment cloned BamHI/XbaI	This study
pAA79	*LEU2, CEN6, ARSH4, UPF1* (genomic promotor)	27
pCM189	*URA3, ampr, lacZ, CEN6, tTA* (tetR promotor moiety)	30
pCM189-EIF5A1	pCM189 containing human *EIF5A1* fragment cloned BamHI/PstI	This study
pCM189-EIF5A1G$_{81}$	pCM189 containing point mutated (V81G) human *EIF5A1* fragment cloned BamHI/PstI	This study

half-life of unspliced *CYH2* mRNA (9). The genetic background of this strain, however, reveals a functional *HYP1* introducing the possibility that it might affect the observed phenotypic effects.

Two studies revealed a connection between eIF5A and senescence processes showing a transcriptional up-regulation of deoxyhypusine synthase and eIF5A in aging tomato plants (21, 22). However, in mammalian IMR-90 cells senescence led to a distinct attenuation of the hypusine formation (23). So far the cellular mechanism by which eIF5A is involved in cell aging is not known.

Using yeast as a model system in which both native *HYP* genes were disrupted we describe the effects of expressing the point mutation V81G in the human hypusine-containing protein eIF5A1. We observed strong temperature sensitivities in these yeast strains. Expression of the mutant protein resulted in the accumulation of nonsense-containing RNAs, which are known to be specifically degraded by the polyadenylation-independent 5′–3′ mRNA decay pathway (nonsense-mediated decay (NMD)[2]). Additionally elongated half-lives of selected NMD transcripts and shortened telomeres were observed. These results suggest a functional connection of eIF5A with the NMD machinery that is coupled to translation initiation and reinforce the notion that the protein might influence essential cellular functions via its role in RNA processing.

EXPERIMENTAL PROCEDURES

Yeast Strains, Plasmids, and Growth Conditions—Yeast cells were grown either on semisynthetic medium with 2% galactose or 2% glucose or on yeast-peptone-dextrose medium and yeast-peptone-galactose medium (24). The plasmid shuffle with and without 5-fluoroorotic acid as selective agent was performed as described previously (25). *S. cerevisiae* strains used in this study are listed in Table 1. The disruption of the *HYP1* gene was performed with the haploid strain WDH#6–9[YEpHYP2] (3) bearing a disruption of *HYP2* by a 2.22-kb *LEU2* fragment. The *HYP1* gene (cloned as a 1.94-kb EcoRI-BamHI fragment in a plasmid derived from pBluescript; Stratagene) was disrupted by insertion of a 1.6-kb SmaI-AatII fragment carrying the *TRP1* marker gene into the single SalI site of the *HYP1* coding region. From the resulting vector a linear 3.6-kb EcoRI-BamHI fragment was used for homologous recombination according to Rothstein (26). Correct integration was verified by Southern analysis. Isolation of high molecular weight genomic yeast DNA, cloning, and *in vitro* mutagenesis of DNA were performed as described previously (24, 31). PCR amplification was used to clone the coding regions of different wild-type and point mutated *HYP* genes according to the properties of multiple cloning sides in the target vectors. The plasmids used and produced for this study are listed in Table 2. The constructs for *HYP* expression either harbored the coding sequence of the *HYP2* gene (*S. cerevisiae*) or the cDNA of the human *HYP1* gene *EIF5A1*. Transformation of yeast strains was performed using the lithium ion method (32).

Anti-eIF5A Western Blotting—To determine eIF5A levels in V81G mutant strains, cells were grown to an A_{600} of 1 at 25 °C or shifted to 37 °C and incubated at this temperature for a further 6 h. SDS-PAGE and immunoblotting were performed as described previously (33) using a 1:10,000 dilution of polyclonal antiserum against human EIF5A1 and enhanced chemiluminescence detection (GE Healthcare).

MTT Cell Viability Test—An MTT viability assay of mutant and wild-type yeast cells was performed as described previously (34).

Terminal Deoxynucleotidyltransferase-mediated dUTP Nick End Labeling (TUNEL)—The TUNEL assay and appropriate cell preparations were performed as described previously (35)

---

[2] The abbreviations used are: NMD, nonsense-mediated decay; FITC, fluorescein isothiocyanate; GAPDH, glyceraldehyde-3-phosphate dehydrogenase; HDOA, high density oligonucleotide array; LTR, long terminal repeat; MTT, 3-(4,5-dimethylthizole-2yl)-2,5-diphenyltetrazolium bromide; ORF, open reading frame; ts, temperature-sensitive; TUNEL, terminal deoxynucleotidyltransferase-mediated dUTP nick end labeling; Ty, transposon yeast; fmk, fluoromethyl ketone; PD, population doubling.

using the *In Situ* Cell Death Detection kit (Roche Applied Science). Coverslips were mounted with a drop of 5% *n*-propyl gallate (Sigma) in glycerol (100%). Slides were analyzed by fluorescence microscopy.

Measurement of Caspase Activation—In vivo staining of caspase activity by flow cytometric analysis was performed as described previously (36) using FITC-VAD-fmk (CaspACE, Promega) and a FACSCalibur system (BD Biosciences). Wild-type cells treated with 3 mM H_2O_2 served as a positive control.

*Generation of Gene Expression Datasets by Microarray Analysis—*For high density oligonucleotide array (HDOA) analysis total RNA was isolated using the hot phenol method (37) from cultures grown at 25 °C reaching early logarithmic phase. For each experiment RNA was independently isolated from four isogenic yeast strains of the wild type and the mutant (strains WDH(hum)Gal and WDHG$_{81}$Gal), and *in vitro* transcriptions and hybridizations were performed. Thus, a total of eight chips were included in the analysis (4 replicates $\times$ 2 datasets for the wild type and the mutant V81G). RNA was further purified with RNeasy columns (Qiagen). In brief 30 μg of total RNA were subjected to a cDNA synthesis reaction to make the first strand using an oligo(dT) primer with a T7 promoter sequence added to the 5′-end. After synthesis of the second strand, double-stranded cDNA was purified by phenol/chloroform extraction, precipitated, and resuspended in nuclease-free water. Biotin-labeled cRNA was made by *in vitro* transcription using the High Yield Transcription kit (ENZO Diagnostics). The resulting cRNA was fragmented at 94 °C for 35 min in buffer A (40 mM Tris acetate, 100 mM KOAc, and 30 mM $Mg(OAc)_2$). Affymetrix yeast S98 GeneChip® arrays were hybridized, washed, stained, and scanned according to the manufacturer's specifications. Scanned raw data images were processed with Affymetrix GeneChip Version 3.2 software.

*Normalization and Statistical Analysis of Hybridization Data—*Data from the arrays was normalized, and expression values based on an additive model were calculated according to the method of Irizarry *et al.* (38). Differentially expressed genes were identified by the permutation-based method of Tusher *et al.* (39). Briefly to control for multiple testing, a false discovery rate (40) was calculated as the percentage of genes falsely detected as differentially expressed among all genes detected as differentially expressed. The *q* value is the lowest false discovery rate at which the gene is called significant. Significant genes were identified if they exhibited the lowest *q* value computed by SAM ("Significance Analysis of Microarrays") software. Detailed information regarding the analysis performed on the microarray data can be found in the supplemental data section. Primary array datasets were published in the gene expression and hybridization array data repository of the National Center for Biotechnology Information (Gene Expression Omnibus (GEO), www.ncbi.nlm.nih.gov/geo/, accession number GSE5290). The transcriptomic profiles of V81G with NMD-deficient yeast were compared with the original .cel files published by He *et al.* (41) and are available at www.ebi.ac.uk/miamexpress/ under accession numbers E-MEXP-26 and E-MEXP-27. These datasets were analyzed in exactly the same way as the microarray data produced for this study.

*Northern Blotting and Determination of mRNA Half-lives—*Yeast strains were cultured until they entered early log phase at either 25 or 37 °C. Total RNA was isolated as before (37). Northern blotting was carried out as described previously (42). RNA was detected by hybridization to digoxigenin-labeled DNA probes of about 350 bp in length that were prepared by PCR using yeast genomic template DNA. After hybridization and stringent washing signal detection was performed using anti-digoxigenin antiserum (Roche Applied Science). Quantification of RNA bands was performed using densitometry. The stability of selected mRNAs was determined according to Parker *et al.* (43). Briefly 200 ml of mutant and wild-type yeast strains were grown to $A_{600} = 0.7$ and incubated for 1 h at either 25 or 37 °C. Next transcription was inhibited by the addition of thiolutin (20 μg/ml), and subsequent samples were taken at 0-, 4-, 8-, 16-, 32-, and 64-min intervals and frozen quickly in a dry ice-ethanol bath. Subsequently total RNA was isolated, and 10 μg of RNA/lane was analyzed by Northern blotting as described above.

*Quantitative Real Time (Reverse Transcriptional) PCR—*Gene-specific primers were designed with the PrimerExpress software (Applied Biosystems). The antisense primers were used for reverse transcription with avian myeloblastosis virus reverse transcriptase (Promega) according to the manufacturer's instructions and using 2 μg of total RNA. Real time PCR was performed using SYBR® Green PCR Master Mix and a Gene-Amp5700 sequence detection system (Applied Biosystems) according to the protocols of the manufacturer. Relative expression levels were calculated, and PCR efficiencies were determined as described previously by Pfaffl (44) and Ramakers *et al.* (45), respectively, using *ACT1* expression for normalization. For each RNA preparation tested a minimum of three independent real time (reverse transcriptional) PCR experiments were conducted.

*Determination of Telomere Length by Southern Analysis—*Telomere lengths were determined as described previously (46). Briefly a probe containing a telomere repeat sequence was prepared by 5′-end labeling of the oligonucleotide Tel-Rep4 (CACCACACCCACACCCACACCACACCCACACACCCA-CAC) with digoxigenin. The sequence was identical to 2.5 repeats of the telomere template sequence from the chromosome 8 analogue to *TLC1*. Total genomic DNA was digested with PstI, and Southern blotting was performed as before. Signal development was achieved by using the DIG (digoxigenin) Luminescent Detection kit (Roche Applied Science) according to the manufacturer's instructions.

RESULTS

*Isolation of the Temperature-sensitive Point Mutant V81G—*To study the relationship between structure and function in the human EIF5A1 hypusine-containing protein point mutations were made throughout the entire length by exchanging phylogenetically conserved residues with related amino acids. A yeast strain was constructed (W303Δh1h2) in which both the genes *HYP2* and *HYP1* (*ANB1*) encoding for the hypusine-containing protein were disrupted (3). The strain harbored a 2μ-*URA3*-plasmid-borne wild-type copy of the genomic *HYP2*, thus complementing the otherwise lethal phenotype. The constructs
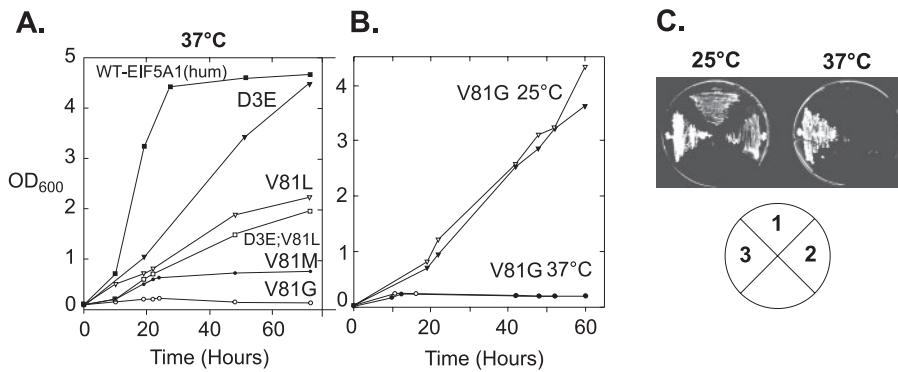
FIGURE 1. **Growth characteristics of yeast strains expressing point mutated forms of human *EIF5A1*.** *A*, growth kinetics at 37 °C of a haploid W303Δh1h2 strain carrying two disrupted *HYP* genes complemented with either wild-type human *EIF5A1* or various point mutants of residue 81 of the human *EIF5A1*. Substitution of Val-81 for Gly led to the strongest growth inhibition. *B*, growth kinetics of the V81G strains (two independently isolated mutant strains) at the permissive (25 °C) and restrictive temperatures. *C*, complementation of the V81G mutated *HYP* with wild-type human *EIF5A1*. *1* and *2*, two isogenic strains expressing the V81G protein; *3*, mutant strain from position 1 retransformed with a single copy plasmid expressing human wild-type *EIF5A1* shows a clear reversibility of the temperature-sensitive phenotype. *WT*, wild-type.
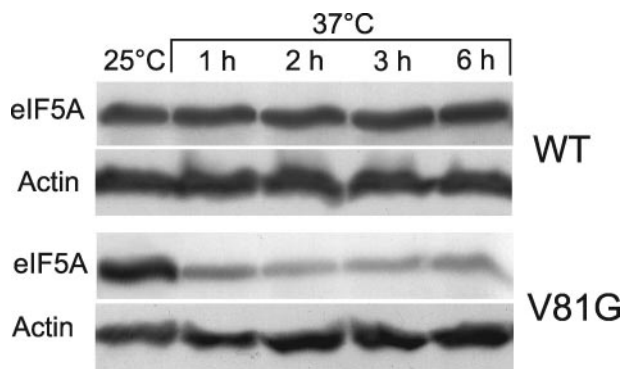

FIGURE 2. **Protein expression of wild-type and V81G mutated human eIF5A in yeast.** Cells were incubated at 25 or at 37 °C for the indicated times and were subsequently harvested to prepare complete cell lysates. Equal amounts of total protein from mutant and wild-type strains were separated by SDS-PAGE. Western blotting was performed with a rabbit polyclonal antiserum against the human EIF5A1 protein. Equal loading of all lanes was confirmed by densitometric scanning of the Coomassie-stained gel prior to blotting as well as quantification of the actin 1 protein on the Western blots that was equally expressed in wild-type and mutant strains. *WT*, wild type.

containing the point mutations to be tested were cloned into pRS313 containing the GAL promotor and transformed into the W303Δh1h2 cells. The exchange of the wild type for a mutated allele was performed by selective plasmid shuffling using fluoroorotic acid. Because hypusine is essential, cell death occurred if the mutant allele cloned in pRS313 was incapable of complementing the gene function of the wild type. This counterselection was used to screen all mutations in the human *HYP* homologue *EIF5A1*.

The expression of certain mutated alleles resulted in temperature-sensitive yeast strains. The strongest temperature sensitivity was observed by the substitution of the valine residue at position 81 (Fig. 1). Proliferation of cells at the restrictive temperature was stopped after only one round of doubling when valine at position 81 was mutated to a glycine (V81G). In comparison with wild type the growth of the mutated strain at the permissive temperature was decelerated. Retransformation of the mutant strains with a single copy plasmid carrying wild-type human *EIF5A1* completely restored the

temperature sensitivity (Fig. 1*C*) indicating that it was not a recessive mutation. Several independent transformations and subsequent 5-fluoroorotic acid selections reproducibly showed the pronounced phenotype of the mutant V81G. These mutated strains were chosen for the subsequent phenotypic characterization experiments.

eIF5A Protein Levels and Viability at 37 °C—Complete cell lysates were prepared from wild-type or mutant cells after incubation at permissive or restrictive temperatures (Fig. 2). The eIF5A protein levels in each case were determined by Western blotting. At 25 °C the mutated protein was expressed to nearly the same amount as the wild type. Within 60 min after heat shock induction the level of the eIF5A (V81G) protein declined more than 5-fold. A further 5-h incubation at 37 °C did not result in further changes in the protein level.

The viability of V81G-expressing cells at both temperatures was checked with an MTT assay (Fig. 3). Independently isolated strains of the mutant V81G and the corresponding wild-type strains that were in early logarithmic growth phase were tested at both the restrictive and the permissive temperatures. Fig. 3 shows that the formation of blue formazan from the activity of dehydrogenases was similar for the wild-type cultures grown at either the restrictive or the permissive temperature. Slight differences were observed between wild-type *HYP2* expression in yeast and heterologous (human) *EIF5A1* expression. However, even at the permissive temperature, V81G, although capable of growth, displayed a 50% reduction in viability when compared with the wild type. After a 6-h incubation at 37 °C the viability was further decreased.

To determine whether the mutant's loss of cell viability was due to apoptotic death a TUNEL assay was performed, and the results are shown in Fig. 4*B*. No fluorescence was detected in the control cells expressing wild-type eIF5A regardless of the growth conditions. However, addition of 3 mM H_2O_2 and incubation for 6 h at 37 °C rendered the cells positive for DNA breaks, which served as a positive control. At the permissive temperature (25 °C) the V81G mutant did not show any fluorescent nuclei. In contrast, after 4 h at the restrictive temperature (37 °C) clear fluorescence in the nuclei was visible and increased with longer incubation times.

To determine whether endogenous caspases were activated in the mutant as a result of the induction of apoptosis a flow cytometric assay was performed. Yeast cells were incubated *in vivo* with FITC-labeled VAD-fmk (FITC-VAD-fmk), which specifically binds to the reactive center of active caspases in eukaryotic cells (36). Fig. 4*Aii* shows that incubation of mutant cultures at 37 °C for 6 h activated caspases in 33% of the counted cells. An equal fraction of apoptotic cells was detected in wild-type cultures in which apoptosis was induced by treatment with 3 mM H_2O_2. In contrast the V81G mutant strain showed no
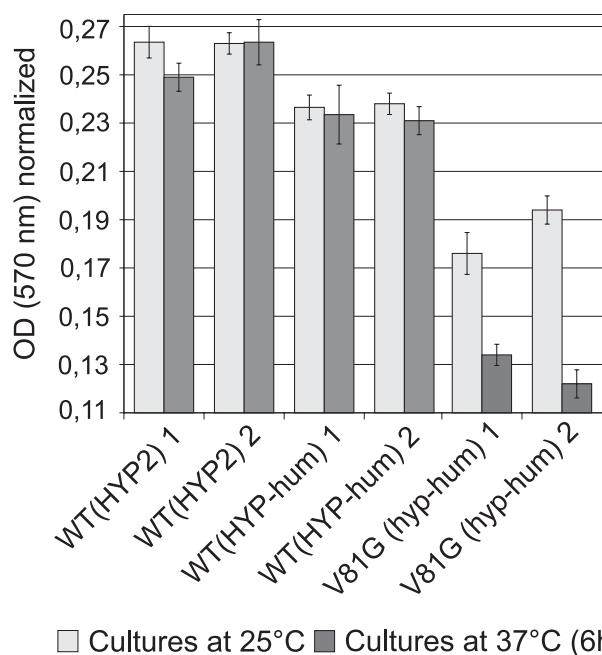
FIGURE 3. **MTT viability assay of mutant and wild-type cultures incubated with MTT for 2 h at the permissive and restrictive temperatures.** Two independently isolated clones of each strain (WDH(hum)TO, WDHyp2TO, and WDHG$_{81}$TO) were tested. Cell density of all cultures was normalized to 5×10^8 cells/ml, and isopropanolic cell extracts were measured at 570 nm. This OD value was proportional to the amount of blue formazan that was formed during reduction time. *Error bars* indicate the standard deviation of triplicate measurements of each of the two isogenic strains. Student's *t* tests for independent samples performed on every pair of strains in all cases generated *p* values below 0.05, indicating significance of the results. *WT*, wild type.

caspase-activated cells in cultures that had been incubated for a shorter time (3 h) at a higher temperature or at 25 °C. Propidium iodide fluorescence can be used to detect cells that have died independently of necrotic or apoptotic triggers. As nearly all propidium iodide-positive cells also showed FITC-VAD-fmk fluorescence (accumulation of cells in the *upper right* region R1 of the dot blot, Fig. 4*Ai* cell death in these cells occurs by apoptosis rather than by necrosis. In summary the results show that incubation at 37 °C but not at 25 °C led to phenotypic effects related to programmed cell death in the V81G strain. Due to the V81G growth characteristics, all subsequent experiments were performed with the V81G strain that had been incubated either at 25 °C or at 37 °C less than 1 h.

Genome-wide Transcriptome Analysis of the Mutant V81G Strain—To identify transcripts regulated by eIF5A, RNA expression profiles of wild-type and V81G strains cultured at the permissive temperature were analyzed. HDOAs were used that covered the whole yeast genome (47). On the array, 9275 probe sets encoding 7839 yeast genes were present of which 6068 genes (6337 probe sets) were coding for proteins, hypothetical proteins, or open reading frames. A group of "further elements" contained 767 probe sets representing rRNA, tRNA, small nucleolar RNA, and small cytoplasmic RNA as well as transcripts derived from Ty retrotransposal RNAs and their LTR sequences were also observed. All probe sets representing mitochondrial encoded transcripts were found among a group of "further ORFs" (Table 3) consisting of 2171 probe sets

including putative or non-annotated ORFs postulated by the yeast genome sequencing project or serial analysis of gene expression.

cRNA probes derived from total RNA preparations were obtained from four isogenic, haploid strains from each of the wild type and the mutant. This ensured that changes in the transcriptome could be attributed to the impaired *HYP* function of V81G rather than to differences in the genetic background. Therefore, two groups of four datasets (per wild-type and mutant strains) were generated after hybridization to the HDOAs. The robust multichip average procedure ("Experimental Procedures") could be used for the normalization of all samples because we showed that the quantification of the absolute RNA amounts that were spiked prior to cDNA synthesis were found to be identical. Transcripts were classified as differentially expressed if they could be assigned to the lowest *q* value of 0.08796% indicating a high level of significance.

In this way the pairwise comparison of the transcriptomes of the V81G and wild-type strains resulted in 604 differentially expressed transcripts (Table 3). 415 (421 probe sets) showed up-regulation, and 188 (205 probe sets) showed down-regulation. These two transcript groups served as the basis for the following evaluations. A functional classification of up- and down-regulated genes and ORFs in V81G mutant strains (according to Ref. 48) can be found in the supplemental data to this study (see supplemental Fig. S1). The temperature shift from 25 to 37 °C and a 3-h period of incubation at high temperature barely had any effect on the distribution of gene functions (data not shown).

Partial Abrogation of the Telomere Position Effect and Enrichment of Ty Retrotransposal RNAs—345 accumulating ORFs in V81G (without those found by serial analysis of gene expression) were analyzed with regard to their chromosomal location. We found that 29.3% of the ORFs in the yeast genome (119 of 406) were within a 27-kb region of the telomeres. These subtelomeric ORFs were up-regulated in the mutant strains. In contrast only 3.4% of the non-telomerically encoded ORFs of the yeast transcriptome (199 of 5863 ORFs; without Ty and LTR elements) were up-regulated. Furthermore a connection between the level of enrichment and the number of telomeric transcripts was seen. Of the 345 ORFs the greatest enrichment was observed for the ORFs closest to the telomeres (subtelomeric), whereas the bulk of the remaining ORFs that showed less enrichment were found further from the telomeres (see Fig. 5).

Genes located nearby chromosomal telomeres are transcriptionally repressed in *S. cerevisiae*. This chromosomal area contains a lower density of ORFs than other regions. The phenomenon was named the telomere positioning effect (49). Normally the telomere positioning effect rapidly decreases as the distance between an ORF and the telomere increases. At every telomere a number of ORFs were found for which transcriptional activity was not altered when compared with the wild type. Thus, referring to the data, the telomere positioning effect in the mutant V81G was reduced but was not completely abolished compared with the wild type.

Retrotransposons and their controlling elements represent 0.9% of the entire ORFs in the whole yeast genome.
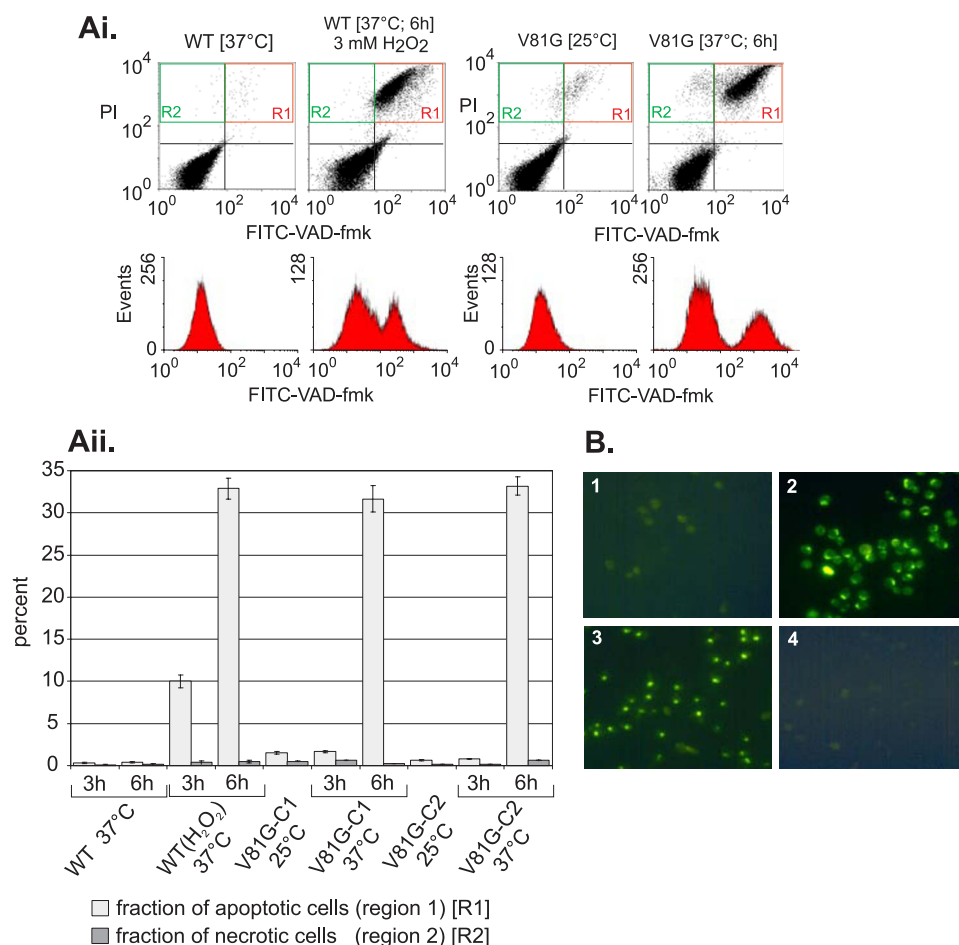
Ai.

Aii.

☐ fraction of apoptotic cells (region 1) [R1]
▨ fraction of necrotic cells   (region 2) [R2]

B.

FIGURE 4. **Test for apoptotic death in growth-arrested cells of V81G.** *A, i* and *ii*, measurement of caspase activation. After cultivation cells from wild-type and V81G strains were stained for active caspases with the caspase substrate FITC-VAD-fmk and analyzed by flow cytometry (*Ai*) counting 25,000 cells of each strain. Treatment of wild-type cultures with 3 mM H_2O_2 for 6 h induced apoptosis in 35% of the cells (positive control) represented by accumulation of cells in the *upper right quadrant* (region 1 (*R1*)) of the dot blot. Staining with propidium iodide (*PI*) enabled the apoptotic fraction to be distinguished from the necrotic fraction (region 2 (*R2*)). Incubation of the V81G strains at 37 °C for 6 h but not at permissive temperature led to the activation of caspases in a fraction of cells that was comparable to that found in the positive control. *Aii*, a quantitative comparison of necrotic and apoptotic cell fractions. *Bars* represent the percentage of the cells counted in regions 1 and 2 from four independent experiments (mean ± S.D.). The results obtained from two isogenic strains of the mutant are included. *B*, TUNEL assay of wild-type and V81G mutated strains. Wild-type cells cultivated at 25 and 37 °C were used as negative controls. *1*, cells of V81G cultured at 25 °C; *2*, V81G cells after incubation at 37 °C for 6 h; *3*, positive control of wild-type cells incubated in the presence of 3 mM H_2O_2 for 6 h at 37 °C; *4*, wild type cultivated at 37 °C (6 h). Only V81G cells incubated at restrictive temperature showed clear fluorescence of nuclei due to antibody detection of double strand breaks of nucleosomic DNA. *WT*, wild type.

When we compared this to the pool of transcripts that were increased in the V81G strain we found that this number increased to 10% of the total transcripts (see supplemental Fig. S1). The number of enriched Ty retrotransposal transcripts including two Ty4 and two Ty3 full-length RNAs and about 40 transcripts coding for LTR elements of all five kinds of retrotransposons (Ty1–5) are shown in Fig. 5 (for details see supplemental data file Array-Data-S4). Of these most LTRs originated from Ty1 and Ty4 elements. Interestingly we observed a significant portion of the accumulating transcripts (15%) near the Ty retrotransposons or LTR sequences remaining from former retrotransposition processes. Especially interesting was a position upstream of the 5′-end of a Ty-LTR that led to accumulation of the RNA of the corresponding adjacent ORF. This points to eIF5A playing a role in processes involving retrotransposons.

Significant Overlap of the V81G-accumulating Transcriptome with Those of Strains Deficient in 5′–3′ mRNA Degradation—We reproducibly found a 4-fold up-regulation of the *UPF2* mRNA. The corresponding protein together with Upf1p and Upf3p function as trans-acting factors of the mRNA NMD pathway. This pathway also includes the mRNA decapping enzymes *DCP1* and *DCP2* and the 5′-exonuclease *XRN1*. Of all genes belonging to the NMD pathway only the *UPF2* tran-

TABLE 3

Numbers of increased and decreased transcripts in the mutant V81G in comparison with the wild-type obtained by microarray analysis

Strain	q^a	Increases				Decreases				Both, total
		ORFs[b]	Further elements[c]	Further ORFs[d]	Subtotal	ORFs	Further elements	Further ORFs	Subtotal	
	%									
eIF5A-V81G-ts	≤0.08796	298	32	85	415	163	4	21	188	604
upf1Δ	≤0.07775	380	39	105	524	38	1	2	41	565
upf2Δ	≤0.06749	376	36	90	502	48	6	9	63	565
upf3Δ	≤0.05349	476	39	121	636	69	13	10	92	728
upf123Δ[e]		529	43	133	705	106	15	18	139	844
dcp1Δ	≤0.01432	664	46	133	843	278	28	35	341	1184
xrn1Δ	≤0.02426	640	41	116	797	361	34	38	433	1230

[a] The q value computed by the SAM (Significance Analysis of Microarrays) software represents the threshold of significance for finding accumulated or decreased transcripts.
[b] ORFs indicates transcripts encoded by protein-coding genes on the chromosomes.
[c] Further elements represents transcripts encoded by genes of rRNAs, tRNAs, small RNAs, and RNAs encoded by transposable elements and their LTRs.
[d] Further ORFs, non-annotated or putative ORFs identified by the genome sequence project and by serial analysis of gene expression as well as genes of DNA plasmids or those encoded on the mitochondrial genome.
[e] *upf123Δ* is the combination of transcriptomic profiles of each of the three *UPF* genes.

scripts showed a changed mRNA level in comparison with the wild type.

Two genome-wide studies of transcriptomic profiles from *UPF123*, *DCP1*, and *XRN1* knock-out yeast strains have been performed (41, 50). The transcriptomes of the eIF5A-ts mutant were compared with NMD-deficient strains using primary microarray data published by He *et al.* (41) by performing the same normalization and statistical analysis procedures with all hybridization datasets.

Knock-out of any of the *UPF* genes resulted in the up-regulation of 705 ORF mRNAs (see Fig. 6, *A* and *B*, *upper left circles*)
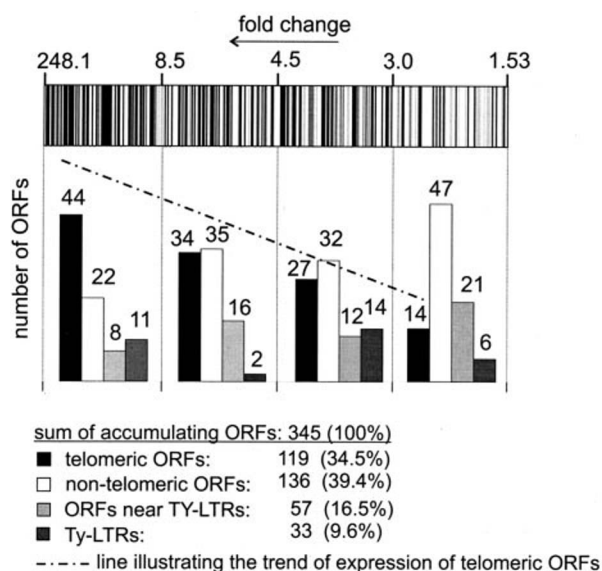

FIGURE 5. **Distribution of telomeric and non-telomeric ORFs within the group of up-regulated transcripts in V81G strains.** The bar code distribution (divided into four parts) represents 345 up-regulated ORFs in the mutant sorted in a descending order for their mean -fold change factors. The number of telomeric ORFs increases with increasing -fold change factors (indicated by the *punctured trend line*). In accordance most transcripts showing slight increases are not positioned near telomeres of chromosomes. Also information about the distribution and number of transcripts of Ty retrotransposons (including their LTR elements) and ORFs being located near Ty elements and Ty-LTRs on the chromosomes is included.
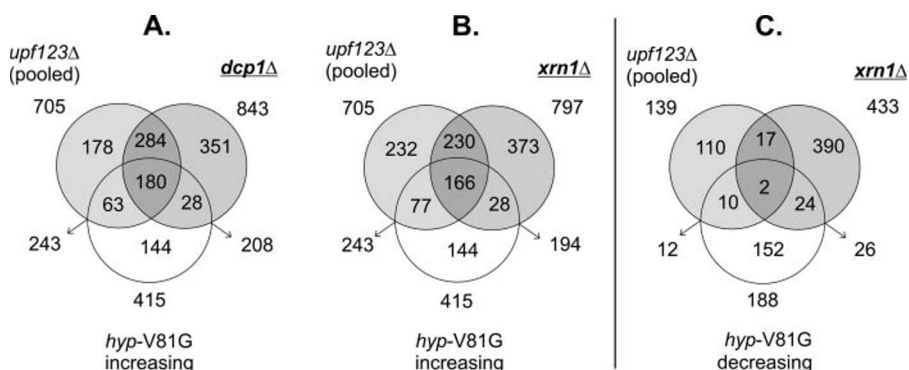
including Ty retrotransposons and their LTRs. On average 139 transcripts were found to be depleted (Fig. 6*C*, *upper left circle*). The *dcp1*Δ and *xrn1*Δ strains showed a higher number of regulated ORFs (Table 3). 843 ORFs in the *dcp1*Δ and 797 in the *xrn1*Δ strains accumulated.

Among the up-regulated RNAs in the V81G strain numerous transcripts overlapped with those up-regulated in strains bearing knock-outs of components in either the NMD or 5′–3′ mRNA degradation pathway, respectively (Fig. 6*A*). 243 transcripts (59%) of the on average 415 increasing ORFs in the mutant were also up-regulated within the pool of up-regulated transcripts of *upf123*Δ strains. Compared with those transcripts up-regulated in *xrn1*Δ/*dcp1*Δ strains the overlap was about 10% lower (208 ORFs in comparison with *dcp1*Δ and 194 ORFs in comparison with *xrn1*Δ strains, representing 50 and 47% of the enriched transcriptome of V81G). Examination of the down-regulated transcripts in NMD and *hyp*-deficient strains showed no significant overlap (Fig. 6*C*).

Determination of mRNA Steady States and Decay Rates—To validate the obtained microarray data and to find evidence that the accumulation of mRNAs in V81G was due to a direct mRNA decay defect in the mutant and not due to indirect effects that influence mRNA levels, mRNA steady states and decay rates of selected transcripts were measured.

The relative levels of nine transcripts found to accumulate in the V81G strain were analyzed by Northern blotting (Fig. 7*A*) and real time (reverse transcriptional) PCR (Fig. 7*B*) after the cells were cultivated at 25 °C. These transcripts were shown to be up-regulated thus supporting the microarray results. Two additional transcripts of factors that function in telomere length control (*EST1* and *STN1*) were quantified and also found to be up-regulated in the mutant. Furthermore mRNA stability was determined for five transcripts (Fig. 7*C*). Specifically the intron containing *CYH2* pre-mRNA, a direct target of NMD, showed only a slightly prolonged half-life in the mutant at the permissive temperature compared with the wild type. After a shift to 37 °C and a further incubation for 1 h the transcript was stabilized with a decay rate decreasing by a factor of 15 (Fig. 7, *left*).

The *ARN1* and *BSC4* transcripts accumulated similarly in V81G and NMD knock-out strains (41). 3–5-fold increased half-lives were determined for both transcripts at 37 °C in the mutant strain. Based on the microarray data the transcripts of the 40 S ribosomal protein S5 (*RPS5*) and GAPDH2 (*TDH2*) served as negative controls. Both transcripts showed no differences in RNA half-lives (Fig. 7*C*) between the wild-type and V81G strains.

Shortening of Telomeres in V81G Mutant Strains—In the eIF5A mutant several mRNA species of genes with functions in the metabolism of telomeres, including the telomerase catalytic subunit encoded by *EST2*, were significantly up-regu-

FIGURE 6. **Overlap between the transcriptomic datasets of the *HYP* mutant V81G and *nmd*Δ yeast strains.** *A* and *B*, overlap of elevated transcriptomes. The *upper left sections* named *upf123*Δ represent the combined number of elevated ORFs in strains carrying disruptions in one, two, or all three *UPF* genes (41). The number of elevated transcripts in *xrn1*Δ or *dcp1*Δ strains is contained in the *upper right sections*. The overlaps of both groups of elevated ORFs in NMD-deficient strains to those measured in the V81G strains are shown. The *arrows* mark the number of overlapping transcripts equally present in two groups of accumulating transcripts. Of 415 significantly up-regulated transcripts in V81G 59% (243) were also up-regulated in the *upf123*Δ, and 50% (208)/47% (194) were up-regulated in the *dcp1*Δ/*xrn1*Δ yeast strains. *C*, the three groups of decreasing transcripts do not show significant overlaps.

lated (see supplemental Table S1). For this reason we wanted to know whether this caused any effect on the telomere metabolism in V81G. Hence the length of the telomeres was compared in the mutant and wild-type strains.

After digestion of genomic DNA isolated from the relevant strains that were incubated at 25 and 37 °C, respectively, a terminal telomere fragment of about 800 bp was released from the bigger telomeric regions (Fig. 8). The band contained Y' telomere-associated sequences that can be probed by Southern blotting using a DNA fragment that included the telomeric $T(G_{1-3}/C_{1-3})A$ repeats. The bigger fragments seen on the blot internally contained other subtelomeric fragments that hybridize to the $T(G_{1-3}/C_{1-3})A$ probe.

As shown previously by other groups (46, 51, 52) the disruption of one or more *UPF* genes causes a reduction of the average telomere length by about 65 bp. This result was reproduced using genomic DNA of a *upf1Δ* strain (Fig. 8, *lane 3*). A complementing *UPF1* plasmid was capable of restoring the shortening in this *upfΔ* strain. V81G mutant strains cultured at 25 °C developed a shortening of telomeres in the same range as the *upfΔ* strains dependent on their population doublings (PDs) (Fig. 8, *lanes 4–8*). Newly isolated V81G strains from 5-fluoroorotic acid screening showed the same telomere length as

wild-type strains of the same age tested in parallel. Shorter telomeres were observed when the PD number of the mutant strains exceeded 25. The connection between the strength of telomeric erosion and the age of the mutant is also supported by the observation of decelerated growth with increasing PDs of a cultured strain (data not shown). Interestingly hardly any telomeric signals were obtained when probing V81G genomic DNA samples that were isolated from cultures incubated at 37 °C for 12 h. This correlates with the observed apoptotic cell death confirmed by TUNEL analysis and caspase activation assays. Taken together, the data suggest that the mutated *HYP* function caused a short telomere phenotype that is similar to that seen when the NMD pathway is inactive.

DISCUSSION

In this work phenotypic effects of a distinct temperature-sensitive point mutated variant of eIF5A were investigated. Valentini *et al.* (20) provided the first evidence for the importance of the proline residue at position 83 in yeast Hyp2p. This region was further investigated in this study using the human protein. Interestingly the analogous proline 82 substitution resulted in a lethal phenotype further underscoring the importance of this residue within the protein. Mutational analysis of neighboring amino acids gave rise to the useful temperature-sensitive mutant V81G. Homology modeling of the tertiary structure of human EIF5A1 (53) revealed that it consists of two domains similar to those known from hyperthermophilic Archaea (54). By way of analogy residue 81 of the human protein is most likely positioned at the beginning of a flexible hinge region connecting both domains. The glycine mutation therefore may change the orientation of both domains with respect to each other possibly bringing about a disturbance in function.

Because of the pivotal cellular role of eIF5A we were interested in gaining more insight into the function of the human protein. A large library of human *EIF5A1* mutants was screened resulting in the discovery of specific temperature-sensitive yeast strains. It is of note that human *EIF5A1* permitted normal growth of yeast cells expressing the allele as the unique source of eIF5A (4, 5). This also indicates that the high degree of conservation of eIF5A ensures the same basic functions of the protein in *S. cerevisiae* and higher eukaryotes.

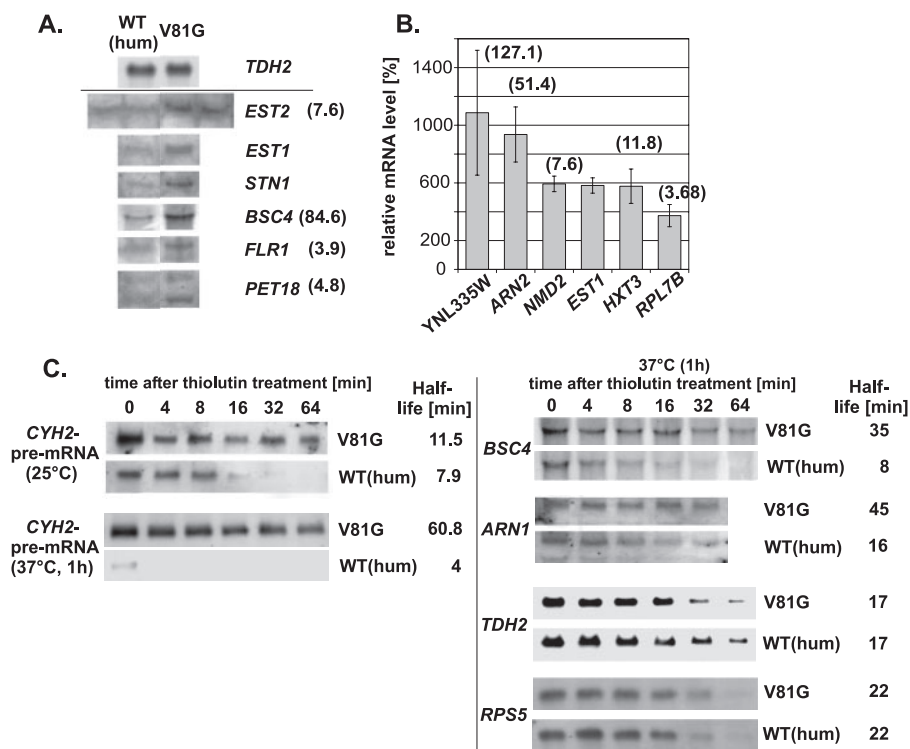To analyze phenotypic effects it was important to test the viability of growth-arrested V81G cells. As

FIGURE 7. **Validation of microarray data.** *A*, determination of mRNA steady states by Northern blotting (cultures grown at 25 °C). Total RNA was extracted and analyzed using probes complementary to six chosen transcripts that showed the highest accumulation in the HDOA analysis (with the exception of *STN1* and *EST1*). Expression levels were normalized to the GAPDH2 (*TDH2*) transcript amount. *B*, real time (reverse transcriptional) PCR quantification of six further genes (ratios are relative to the wild type). The *ACT1* mRNA served as a housekeeping gene. *Bold numbers* in *parentheses* correspond to the accumulation factor of each mRNA generated by microarray analysis. *C*, measurement of mRNA half-lives. Cultures from wild-type and mutant strains were incubated at 37 or 25 °C for 1 h. 20 μg/ml thiolutin was added, and the total RNA was extracted from culture aliquots taken at the times indicated. Northern blotting was performed using 12 μg of RNA/lane. Digoxigenin-labeled DNA probes complementary to about 350 bp of the five target RNAs were used including an intron containing the *CYH2*-pre mRNA and two accumulating transcripts found by the HDOA analysis of V81G (mRNAs of *BSC4* and *ARN1*). The mRNAs of glyceraldehyde-3-phosphate dehydrogenase 2 (*TDH2*) and 40 S ribosomal protein S5 (*RPS5*) served as negative controls. *WT*, wild type; *hum*, human.
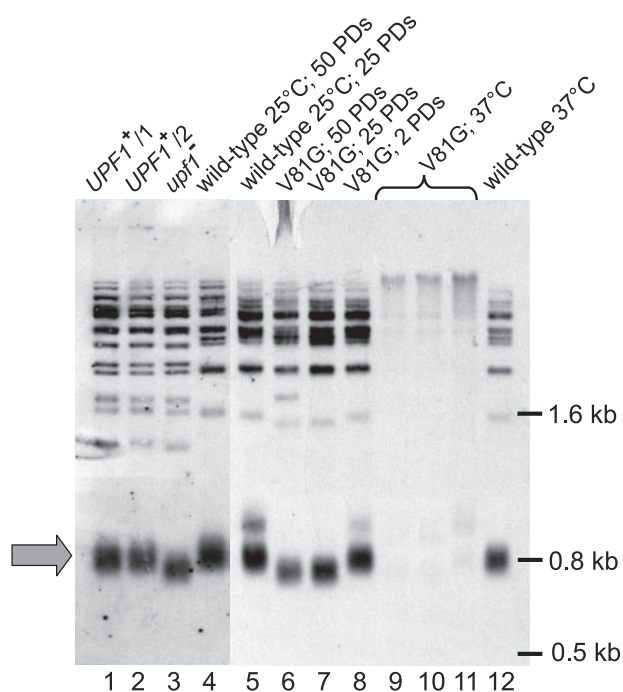
FIGURE 8. **Comparison of telomere length.** V81G mutant strains exhibit shortened telomere tracts depending on their number of PDs after isolation. Total genomic DNA was digested with PstI, and fragments were separated on a 1% agarose gel before blotting. Detection of bands by chemiluminescence was achieved using a dioxigenin-5′-labeled oligo as a probe against a telomere repeat sequence and an anti-digoxigenin peroxidase-coupled antibody. The *arrow* indicates a fragment of ~800 bp that contains 520 bp of the Y′ telomere-associated sequence and about 280 bp of the telomere repeat sequence T(G_{1-3}/C_{1-3})A. *Lanes 1* and *2*, two clones of upf1⁻ strain PLY118 retransformed with the single copy plasmid pAA79 bearing a functional *UPF1* gene; *lane 3*, PLY118 transformed with the empty pAA vector; *lanes 4* and *5*, wild-type strains WDH(hum)Gal expressing human *EIF5A1* cultured for 50 or 25 PDs at 25 °C; *lanes 6–8*, WDH(G_{81})Gal mutant strains expressing human *EIF5A1* carrying the V81G point mutation cultured for 50, 25, or two PDs at 25 °C; *lanes 9–11*, same strains as in the previous lanes, but the cultures were incubated at 37 °C for 12 h; *lane 12*, wild-type strain WDH(hum)Gal incubated at 37 °C for 12 h.

shown in Fig. 3 a significant reduction was shown after 6 h at 37 °C. At the same time the mutant showed initial signs of DNA fragmentation and activation of caspases, which are diagnostic markers of apoptotic death (35, 55). Other researchers have also demonstrated the involvement of eIF5A in the apoptotic processes (56, 57). The induction of apoptosis is often linked to the control of the cell cycle and the DNA damage checkpoint. Several indications exist that eIF5A is involved in cell cycle progression from G_1 to S phase (11, 58). Notably V81G cells at the restrictive temperature showed characteristics of cells arresting in the G_1 phase of the cell cycle as indicated by their bud formation (data not shown). Therefore, a connection between the apoptotic behavior of V81G and the cell cycle arrest seems probable. Further experiments are needed to gain more insight into the apoptotic mechanism in these strains. However, correlation of the strongly reduced protein level of mutated eIF5A after incubation for 1 h at 37 °C with a loss of viability is most likely one of the triggers of the ts phenotype and of the induction of apoptotic death.

Interestingly the addition of up to 1 M sorbitol to the medium caused hyperosmolarity but neither reduced the temperature sensitivity nor altered growth behavior of the mutant. This is in

contrast to the properties of the proline mutants published by Valentini *et al.* (20) who showed a significant attenuation of temperature sensitivity with the addition of sorbitol. The authors of that study suggested an involvement in the *PKC1*-dependent signaling pathway for cell wall integrity. Our results rather indicate different or additional effects of the V81G mutant on the eIF5A function.

Transcriptome analysis revealed ~60% overlap of the up-regulated mRNA molecules in V81G and NMD-deficient yeast strains. Many of these overlapping transcripts could be assigned to known substrate classes of NMD (41, 50). These groups include Ty retrotransposal RNAs, their LTRs, and mRNAs possessing disabling elements. Among these are genes requiring +1 frameshifts or containing premature stop codons that are not caused by nonsense mutations (*e.g.* BSC4 and BSC5). These findings point to a functional connection between the eIF5A function and the 5′–3′-directed mRNA degradation pathway including the nonsense-mediated decay pathway. The microarray data from the NMD knock-out strains indicated that this pathway not only degrades nonsense transcripts of which the translation would lead to potentially harmful truncated proteins but also regulates the activity of a subset of normal yeast genes. A significant portion of the mRNAs from these genes were up-regulated in the V81G strain (see supplemental data for details).

These results are in line with findings that a C-terminal point mutant of Hyp2p showed a strong stabilization of the intron containing the *CYH2* pre-mRNA (9). In addition a 30% reduction in the rate of protein synthesis was observed. The accumulation of RNAs lacking the 5′-cap proposed a function for eIF5A in general mRNA degradation downstream of the decapping step. The number of overlapping ORFs with the core transcripts of the *upf123Δ* strains was about 10% higher than those of *xrn1Δ* and *dcp1Δ* strains (Fig. 6). However, further experiments will be necessary to clarify the exact role of eIF5A within the pathway. At least one-third of the accumulating transcripts from the V81G strain were not found among those of NMD-deficient strains. The hypusine-containing protein has been found to be essential in yeast, whereas the knock-out of NMD does not lead to a cell cycle arrest and apoptotic death. These facts are strongly suggestive of the involvement of eIF5A in further biological processes.

The accumulation of nonsense transcripts and the stabilization of the *CYH2* pre-mRNA were already detected at the permissive temperature. A short incubation time of 60 min at 37 °C was sufficient to increase the *CYH2* half-life by a factor of 15. These facts suggest that the mRNA degradation deficiency is a direct rather than an indirect effect. Measurement of mRNA steady states of selected transcripts confirmed the results obtained by the HDOA analysis (Fig. 7). Evidence that these elevated mRNA levels in the mutant were related to a defect in the Upf-dependent mRNA decay pathway was supplied by the determination of the mRNA half-lives of three NMD-dependent transcripts. The *TDH2* and *RPS5* mRNAs were not found among the group of elevated RNAs, neither in the NMD-deficient strains nor in the V81G strain, and did not show delayed decay. These findings contradict the interpretation that a general defect in mRNA degradation is present in the mutant.

V81G strains displayed a distinct impairment of the telomere positioning effect. In addition the microarray analysis also revealed the accumulation of transcripts of genes playing a direct role in the metabolism of telomeres and of the catalytic subunit of the telomerase itself (supplemental Table S1). We also showed that the V81G mutation leads to a short telomere phenotype (Fig. 8). The same observations were described for NMD-deficient yeast strains that also develop a shortening of telomeres in the range seen in V81G strains.

There is solid evidence that the NMD pathway is essential for telomere metabolism and telomerase function in yeast (51, 52, 46) and that several genes that control telomerase activity like *STN1*, *EST3*, and *EST1* are regulated by NMD as well (51). The *EST1* and *EST2* transcripts were found to accumulate, and the *EST1* mRNA was found to be stabilized in V81G cells. Additionally it is known that increased levels of telomerase-regulating genes cause short telomere phenotypes, and overexpression of *STN1* and *EST2* leads to reduced telomeric silencing (51) similar to that seen in V81G. Therefore, the results strongly suggest that the telomeric effects caused by the eIF5A mutation could be explained via the influences of eIF5A on the NMD pathway, disturbing the natural expression levels of telomerase-regulating genes. Another possibility that is not mutually exclusive to this would be that the stabilization of special transcripts could lead to a down-regulation of translation of their corresponding proteins causing a lack of function of these genes and leading to a dysfunctional telomerase or reduced telomeric silencing.

As the mutant form of eIF5A was expressed at a level comparable to the wild type at 25 °C (Fig. 2) the telomeric effects cannot be due to a decreasing eIF5A protein amount but point to further effects caused by the mutant already at the permissive temperature. Thus, the results gained from V81G at this temperature are relevant even if they do not obviously contribute to its strong temperature sensitivity.

There is evidence for eIF5A involvement in cellular senescence (21, 22, 23). We observed that the growth of the V81G mutant cells significantly decelerated with increasing population doublings indicative of a senescent phenotype. Yeast strains deficient in expressing the telomerase cofactors *EST1* and *EST3*, which are both substrates of NMD, also show characteristics of accelerated aging (59). This points to the involvement of eIF5A in the senescence processes that could be explained by its NMD-dependent regulatory effect on telomere maintenance.

In all Archaea investigated so far deoxyhypusine synthase and eIF5A have been found to be highly conserved proteins indicating a related function for both proteins in Archaea and eukaryotes. Upf1p is a highly conserved RNA helicase in the NMD pathway, and it is highly likely that it has evolved from an ancient ancestor of Archaea and eukaryotes (60), and RNA metabolism itself is conserved in all eukaryotic systems (61). This points to a co-evolution of eIF5A and NMD proteins and suggests a functional connection between these factors.

The observed partial reduction of translation when depleting eIF5A in yeast (8, 9) raised the hypothesis that eIF5A might have a role in the translation/degradation of a specific subset of mRNAs. Further work is needed to prove whether this subset

overlaps with the group of genes regulated by NMD. eIF5A would therefore influence the stability of a section of these NMD-dependent mRNAs before translation. The recognition of nonsense mutations and initiation of translation are intimately linked processes located at ribosomes. It is thus all the more interesting that eIF5A has been found to interact with the ribosomal protein L5 (62). In addition the direct interaction with translating 80 S ribosomes dependent on RNA and the hypusine modification has recently been shown (63).

In summary the eIF5A function is slowly beginning to yield to current molecular biological analysis. In the future elucidating the detailed mechanistic connection of eIF5A and NMD will be of great interest.

REFERENCES

1. Park, M. H. (2006) *J. Biochem.* **139,** 161–169
2. Sasaki, K., Abid, M. R., and Miyazaki, M. (1996) *FEBS Lett.* **384,** 151–154
3. Wöhl, T., Klier, H., Ammer, H., Lottspeich, F., and Magdolen, V. (1993) *Mol. Gen. Genet.* **241,** 305–311
4. Magdolen, V., Klier, H., Wöhl, T., Klink, F., Hirt, H., Hauber, J., and Lottspeich F. (1994) *Mol. Gen. Genet.* **244,** 646–652
5. Schwelberger, H. G., Kang, H. A., and Hershey, J. W. (1993) *J. Biol. Chem.* **268,** 14018–14025
6. Kemper, W., Berry, K., and Merrick, W. (1976) *J. Biol. Chem.* **251,** 5551–5557
7. Thomas, A., Goumans, H., Amesz, H., Benne, R., and Voorma, H. O. (1979) *Eur. J. Biochem.* **98,** 329–337
8. Kang, H. A., and Hershey, J. W. B. (1994) *J. Biol. Chem.* **269,** 3934–3940
9. Zuk, D., and Jacobson, A. (1998) *EMBO J.* **17,** 2914–2925
10. Liu, Y. P., Nemeroff, M., Yan, Y. P., and Chen, K. Y. (1997) *Biol. Signals* **6,** 166–174
11. Hanauske-Abel, H. M., Slowinska, B., Zagulska, S., Wilson, R. C., Staiano-Coico, L., Hanauske, A. R., McCaffrey, T., and Szabo, P. (1995) *FEBS Lett.* **366,** 92–98
12. Jin, B. F., He, K., Hu, M. R., Yu, M., Shen, B. F., and Zhang, X. M. (2003) *Zhongguo Shi Yan Xue Ye Xue Za Zhi* **11,** 325–328
13. Shi, X. P., Yin, K. C., Ahern, J., Davis, L. J., Stern, A. M., and Waxman, L. (1996) *Biochim. Biophys. Acta* **1310,** 119–126
14. Chatterjee, I., Gross, S. R., Kinzy, T. G., and Chen, K. Y. (2006) *Mol. Gen. Genet.* **275,** 264–276
15. Bevec, D., Jaksche, H., Oft, M., Wöhl, T., Himmelspach, M., Pacher, A., Schebesta, M., Koettnitz, K., Dobrovnik, M., Csonga, R., Lottspeich, F., and Hauber, J. (1996) *Science* **271,** 1858–1860
16. Rosorius, O., Reichart, B., Kratzer, F., Heger, P., Dabauvalle, M., and Hauber, J. (1999) *J. Cell Sci.* **112,** 2369–2380
17. Ruhl, M., Himmelspach, M., Bahr, G. M., Hammerschmid, F., Jaksche, H., Wolff, B., Aschauer, H., Farrington, G. K., Probst, H., and Bevec, D. (1993) *J. Cell Biol.* **123,** 1309–1320
18. Jao, D. L.-E., and Chen, K. Y. (2002) *J. Cell. Biochem.* **86,** 590–600
19. Lipowski, G., Bischoff, F. R., Schwarzmaier, P., Kraft, R., Kostka, S., Hartmann, E., Kutay, U., and Göhrlich, D. (2000) *EMBO J.* **16,** 4362–4371
20. Valentini, S. R., Casolari, J. M., Oliveira, C. C., Silver, P. A., and McBride, A. E. (2002) *Genetics* **160,** 393–405
21. Wang, T.-W., Lu, L., Wang, D., and Thompson, J. E. (2001) *J. Biol. Chem.* **276,** 17541–17549
22. Wang, T. W., Lu, L. G., Zhang, C., Taylor, C., and Thompson, J. E. (2003) *Plant Mol. Biol.* **52,** 1223–1235

23. Chen, Z. P., and Chen, K. Y. (1997) *J. Cell Physiol.* **170,** 248–254

24. Sherman, F., Fink, G. R., and Hicks, J. B. (1986) *Methods in Yeast Genetics: A Laboratory Manual*, Cold Spring Harbor Laboratory Press, Cold Spring Harbor, NY

25. Boeke, J. D., Trueheart, J., Natsoulis, G., and Fink, G. R. (1987) *Methods Enzymol.* **154,** 164–175

26. Rothstein, R. J. (1983) *Methods Enzymol.* **101,** 202–211

27. Atkin, A. L., Schenkman, L. R., Eastham, M., Dahlseid, J. N., Lelivelt, M. J., and Culbertson, M. R. (1997) *J. Biol. Chem.* **272,** 22163–22172

28. Hill, J. E., Myers, A. M., Koerner, T. J., and Tzagoloff, A. (1986) *Yeast* **2,** 163–167

29. Sikorski, R. S., and Hieter, P. (1989) *Genetics* **122,** 19–27

30. Garí, E., Piedrafita, L., Aldea, M., and Herrero, E. (1997) *Yeast* **13,** 837–848

31. Sambrook, J., Fritsch, E. F., and Maniatis, T. (1989) *Molecular Cloning: A Laboratory Manual*, 2nd Ed., Cold Spring Harbor Laboratory Press, Cold Spring Harbor, NY

32. Schiestl, R. H., and Gietz, R. D. (1989) *Curr. Genet.* **16,** 339–346

33. Knop, M., Siegers, K., Pereira, G., Zachariae, W., Winsor, B., Nasmyth, K., and Schiebel, E. (1999) *Yeast* **15,** 963–972

34. Hodgson, V., Walker, G. M., and Button, D. (1994) *FEMS Microbiol. Lett.* **120,** 201–206

35. Madeo, F., Fröhlich, E., and Froehlich, K.-U. (1997) *J. Cell Biol.* **139,** 729–734

36. Madeo, F., Herker, E., Maldener, C., Wissing, S., Laechelt, S., Herlan, M., Fehr, M., Lauber, K., Sigrist, S. J., Wesselborg, S., and Froehlich, K.-U. (2002) *Mol. Cell* **9,** 911–917

37. Sprague, G. F., Jr., Jensen, R., and Herskowitz, I. (1983) *Cell* **32,** 409–415

38. Irizarry, R. A., Bolstad, B. M., Collin, F., Cope, L. M., Hobbs, B., and Speed, T. P. (2003) *Nucleic Acids Res.* **31,** 1–8

39. Tusher, V. G., Tibshirani, R., and Gilbert, C. (2001) *Proc. Natl. Acad. Sci. U. S. A.* **98,** 5115–5121

40. Benjamini, Y., and Hochberg, Y. (1995) *R. Stat. Soc. Ser. B* **57,** 289–300

41. He, F., Li X., Spatrick, P., Casillo, R., Dong, S., and Jacobson, A. (2003) *Mol. Cell* **12,** 1439–1452

42. Hatfield, L., Beelman, C. A., Stevens, A., and Parker, R. (1996) *Mol. Cell. Biol.* **16,** 5830–5838

43. Parker, R., Herrick, D., Peltz, S. W., and Jacobson, A. (1991) in *Guide to Yeast Genetics and Molecular Biology* (Guthrie, C., and Fink, G. R., eds) Vol. 194, pp. 415–423, Academic Press, San Diego, CA

44. Pfaffl, M. W. (2001) *Nucleic Acids Res.* **29,** 2002–2007

45. Ramakers, C., Ruijter, J. M., Deprez, R. H., and Moorman, A. F. (2003) *Neurosci. Lett.* **339,** 62–66

46. Lew, J. E., Enomoto, S., and Berman, J. (1998) *Mol. Cell. Biol.* **18,** 6121–6130

47. Wodicka, L., Dong, H., Mittmann, M., Ho, M. H., and Lockhart, D. J. (1997) *Nat. Biotechnol.* **15,** 1359–1367

48. Mewes, H. W., Frishman, D., Güldener, U., Mannhaupt, G., Mayer, K., Mokrejs, M., Morgenstern, B., Münsterkoetter, M., Rudd, S., and Weil, B. (2002) *Nucleic Acids Res.* **30,** 31–34

49. Gottschling, D. E., Aparicio, O. M., Billington, B. L., and Zakian, V. A. (1990) *Cell* **63,** 751–762

50. Lelivelt, M. J., and Culbertson, M. R. (1999) *Mol. Cell. Biol.* **19,** 6710–6719

51. Dahlseid, J. N., Lew-Smith, J., Lelivelt, M. J., Enomoto, S., Ford, A., Desruisseaux, M., McClellan, M., Lue, N., Culbertson, M. R., and Berman, J. (2003) *Eukaryot. Cell* **2,** 134–142

52. Enomoto, S., Glowczewski, L., Lew-Smith, J., and Berman, J. G. (2004) *Mol. Cell. Biol.* **24,** 837–845

53. Facchiano, A. M., Stiuso, P., Chiusano, M. L., Caraglia, M., Giuberti, G., Marra, M., Abbruzzese, A., and Colonna, G. (2001) *Protein Eng.* **14,** 881–890

54. Kim, K. K., Hung, L.-W., Yokorta, H., Okota Kim, R., and Kim, S.-H. (1998) *Proc. Natl. Acad. Sci. U. S. A.*, **95,** 10419–10424

55. Burhans, W. C., Weinberger, M., Marchetti, M. A., Ramachandran, L., D'Urso, G., and Huberman, J. A. (2003) *Mutat. Res.* **532,** 227–243

56. Caraglia, M., Marra, M., Giuberti, G., D'Alessandro, A. M., Budillon, A., del Prete, S., Lentini, A., Beninati, S., and Abruzzese, A. (2001) *Amino Acids* **20,** 91–104

57. Taylor, C. A., Senchyna, M., Flanagan, J., Joyce, E. M., Cliche, D. O., Boone, A. N., Culp-Stewart, S., and Thompson, J. E. (2004) *Investig. Ophthalmol. Vis. Sci.* **45,** 3568–3576

58. Park, M. H., Lee, Y. B., and Joe, Y. A. (1997) *Biol. Signals* **6,** 115–123

59. Lendvay, T. S., Morris, D. K., Sah, J., Balasubramanian, B., and Lundblad, V. (1996) *Genetics* **144,** 1399–1412

60. Culbertson, M. R., and Leeds, P. F. (2003) *Curr. Opin. Genet. Dev.* **13,** 207–214

61. Anantharaman, V., Koonin, E. V., and Aravind, L. (2002) *Nucleic Acids Res.* **30,** 1427–1464

62. Schatz, O., Oft, M., Dascher, C., Schebesta, M., Rosorius, O., Jaksche, H., Dobrovnik, M., Bevec, D., and Hauber, J. (1998) *Proc. Natl. Acad. Sci. U. S. A.* **95,** 1607–1612

63. Jao, D. L., Chen, K. Y. (2006) *J. Cell. Biochem.* **97,** 583–598